# Analysis of the conserved glycosylation site in the nicotinic acetylcholine receptor: potential roles in complex assembly

**Keith W Rickert and Barbara Imperiali***

Division of Chemistry and Chemical Engineering, California Institute of Technology, Pasadena, CA 91125, USA

**Background:** Assembly of the functional nicotinic acetylcholine receptor (nAChR) is dependent on a series of exquisitely coordinated events including polypeptide synthesis and processing, side-chain elaboration through post-translational modifications, and subunit oligomerization. A 17-residue sequence that includes a cystine disulfide and an *N*-linked glycosylation site is conserved in the extracellular domain of each of the nAChR subunits, and is involved in intersubunit interactions that are critical for assembly of intact, pentameric complexes. A polypeptide representing the relevant sequence from the α-subunit of the nAChR (Ac-Tyr-Cys-Glu-Ile-Ile-Val-Thr-His-Phe-Pro-Phe-Asp-Gln-Gln-Asn-Cys-Thr-$NH_2$) is small enough to allow detailed structural analysis, which may provide insight into the role of glycosylation in the maturation process that leads to ion-channel assembly. We therefore investigated the effect of *N*-linked glycosylation on the structure of this heptadecapeptide.

**Results:** Thermodynamic analysis shows that glycosylation alters disulfide formation in the loop peptide, shifting the equilibrium in favor of the disulfide. Spectroscopic studies reveal that the *cis/trans* amide isomer ratio of the proline is also affected by the modification, with a resultant shift in the equilibrium in favor of the *trans* isomer, even though the proline is several residues removed from the glycosylation site. Two-dimensional NMR analysis of the glycopeptide does not indicate the presence of any specific interactions between the carbohydrate and the peptide.

**Conclusions:** These studies demonstrate that glycosylation can have a significant influence on disulfide formation and proline isomerization in a local peptide sequence. As both these processes are considered slow steps in protein folding, it is evident that *N*-linked glycosylation has important indirect roles that influence the folding of the receptor subunit and assembly of the pentameric complex.

**Chemistry & Biology** November 1995, **2**:751–759

Key words: glycosylation, protein folding, conformation

## Introduction

Protein glycosylation is an essential part of the process of protein synthesis, folding and post-translational modification in eukaryotic cells. Asparagine-linked (*N*-linked) glycosylation, in particular, and the resulting glycopeptides and glycoproteins have been the subjects of a great deal of study [1]. It remains a significant problem in biochemistry, however, to understand the biological consequences and functions of *N*-linked glycosylation. Some of the roles ascribed to these modifications include protein targeting, protection of protease sensitive sites, modulation of immunogenicity, and intercellular recognition.

A number of studies suggest that glycosylation can affect protein structure. In some cases, glycosylation has been shown to stabilize the fully folded protein structure [2–4]. Even when glycosylation has little or no influence upon the final structure, it can have a very significant effect upon the kinetics of protein folding [5,6]. In fact, participation in protein folding may be one of the most important functions of *N*-linked glycosylation. The initial attachment of a carbohydrate to the protein occurs co-translationally, as newly synthesized, unfolded proteins are being translocated across the endoplasmic reticulum (ER) membrane and into the lumen of the ER. At this point in the protein synthesis process, *N*-linked glycosylation can significantly influence the course of protein folding by changing the local conformational tendencies of the protein, and several studies have indeed shown distinct conformational consequences of glycosylation on small peptides [7–10].

Many multimeric proteins have specific, highly conserved glycosylation sites. Site-directed mutagenesis studies have implicated these sites in the processes of protein folding and oligomerization. One protein containing such sites is the nicotinic acetylcholine receptor (nAChR) (see Fig. 1 for a schematic drawing of the nAChR architecture) [11]. A highly conserved feature of each of the homologous subunits of the nAChR is a 15-residue loop peptide with the consensus sequence Cys-Xaa-Xaa-Xaa-Val-Xaa-Xaa-Phe-Pro-Phe-Asp-Xaa-Gln-Asn-Cys-Thr/Ser. This polypeptide forms part of the soluble, extracellular domain of the protein and is thought to be involved in intersubunit interactions that are critical for the assembly of intact, pentameric complexes. The loop sequence in the mature α-1 subunit of the neuromuscular nAChR from *Torpedo californica* comprises residues 128–143, including an *N*-linked glycosylation site (Asn-Cys-Thr) flanking one of the cysteines (Cys142), and a proline (Pro136) at the remote end of the loop formed by the disulfide. The intermediate size

*Corresponding author.

 ISSN 1074-5521

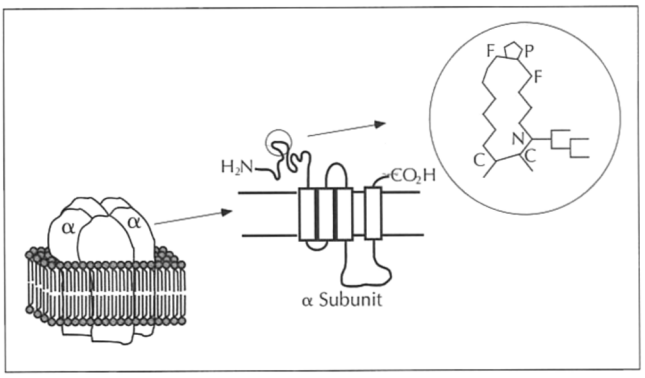


**Fig.1.** The organization of the nicotinic acetylcholine receptor. Left: the receptor is composed of five transmembrane subunits (including two α subunits), which form an ion channel. Middle: The α subunit has four transmembrane domains. The position of the conserved peptide loop in the extracellular domain is circled and is shown in detail on the right.

of the polypeptide renders it amenable to detailed structural analysis, providing insight into the role of this loop in receptor complex assembly and into the importance of the conserved glycosylation site in this process. Although glycosylation of this site has been shown to be essential for proper assembly and for stability of the receptor complex [12–14], the mechanism by which glycosylation influences the structure of the complex is unknown. If *N*-linked glycosylation is important for correct folding of the α-subunit of this receptor, then it may act by producing significant changes in the conformation of the loop. We report here a study of the influence of *N*-linked glycosylation on the conformation of a peptide that corresponds to the nAChR loop containing the conserved *N*-linked glycosylation site.

## Results and discussion

The glycopeptide **2a** (Fig. 2) was prepared by oligosaccharyl transferase catalyzed glycosylation of synthetic peptide **1a** using $^{3}$H-labeled dolichylpyrophosphoryl (Dol-PP)-*N*,*N*'-diacetylchitobiose as the disaccharide donor [8], or by chemical synthesis in which the chitobiosyl amine is coupled to a polypeptide bound to a solid support [15,16]. The glycosylated peptide is modified with a truncated disaccharide (two *N*-acetylglucosamine moieties, $GlcNAc_2$) in lieu of the tetradecasaccharide ($GlcNAc_2Man_9Glc_3$) normally present *in vivo* [1] (see Fig. 2). The biosynthetic preparation of the glycopeptide offered the opportunity to assess the glycosyl acceptor properties of both the reduced and oxidized forms of the loop peptide, and also provided a radiolabeled standard as a reference for the synthetic preparation. The chemical synthesis of the glycopeptide afforded mg quantities of homogeneous material for detailed spectroscopic analysis.

### Effect of disulfide formation on oligosaccharyl transferase activity

The conformation of a peptide is an important determinant of whether it is a good substrate for oligosaccharyl transferase [17,18]. Consequently, disulfide bond formation may influence the capacity of peptide **1** to serve as a substrate for this enzyme. To optimize enzymatic synthesis of the glycopeptide, samples of both the reduced and oxidized peptide were assayed for oligosaccharyl transferase activity. $K_M$ and relative $V_{max}$ values were obtained, and are summarized in Table 1. Formation of the disulfide bond clearly impairs glycosylation of peptide **1**, by both weakening the binding to the enzyme six-fold, and reducing the maximal enzyme velocity, giving an overall decrease of $V_{max}/K_M$ by 8.2. This result is consistent with

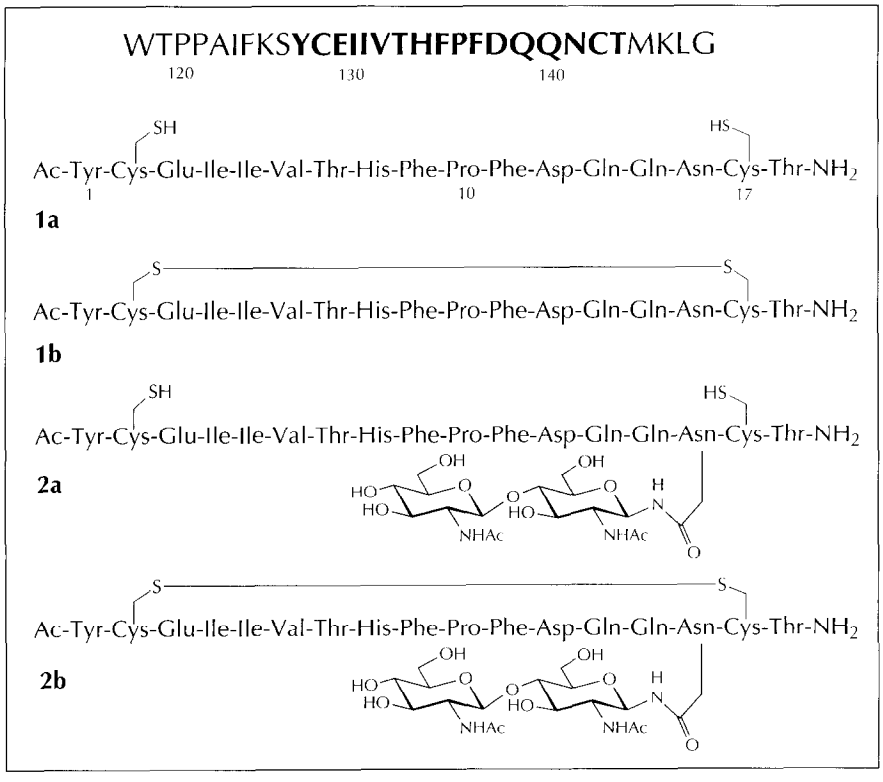


**Fig. 2.** The amino-acid sequences and modifications of the loop peptides from the α-subunit of the *Torpedo californica* nicotinic acetylcholine receptor. Partial sequence of the mature receptor protein is shown above in single-letter code, with the residues studied in boldface. Sequences of the non-glycosylated peptide, **1**, and the glycosylated peptide **2**, in both reduced (**1a** and **2a**) and oxidized (**1b** and **2b**) forms are shown below in three-letter code.

**Table 1.** Kinetic constants of peptides as substrates for porcine liver oligosaccharyl transferase.

| Substrate | Relative $V_{max}$ (dpm/min) | $K_M$ (μM) |
|---|---|---|
| Peptide **1a** (reduced) | 5259 | 36 |
| Peptide **1b** (oxidized) | 3563 | 201 |
| Bz-NLT-NHMe | 7362 | 554 |

Benzoyl-Asn-Leu-Thr-NHMe (BzNLT-NHMe) is included as a standard.

the proposal that the preferred conformation for efficient enzymatic *N*-linked glycosylation is the Asx-turn, with a hydrogen bond between the side chain of an aspartate or asparagine residue and the peptide backbone [18]. Oxidation to the disulfide (peptide **1b**) would be expected to disrupt Asx-turn formation, since one of the two cysteines involved occupies the central position in the -Asn-Xaa-Thr- triad, which is the consensus sequence for formation of this structure. Modeling studies show that an Asx-turn can still be formed by the oxidized peptide, however, and in fact this peptide shows limited glycosyl acceptor properties.

It has been shown that *N*-linked glycosylation takes place shortly after translocation into the ER [19], often before a protein is fully folded [20,21]. Since the nascent polypeptide is not ready for disulfide bond formation until both cysteine residues have fully emerged into the oxidizing environment of the ER, it is probable that disulfide bond formation occurs after glycosylation. The kinetic data for the reduced and oxidized peptides support a model in which *N*-linked glycosylation precedes disulfide bond formation. Peptide **1** (and presumably the α-subunit from which the sequence was derived) is thus well engineered for effective processing, as glycosylation is significantly more efficient prior to disulfide formation.

### Thermodynamics of disulfide formation

The polypeptide loop contains a disulfide bond between Cys128 and Cys142 in the mature protein, which has been shown to be essential for proper subunit folding and receptor complex assembly [13,14,22]. The free energy associated with formation of an intramolecular disulfide can be indicative of the conformation of that molecule, since preorganization to a conformation which places the cysteine sulfhydryls in close proximity lowers the entropic cost of forming the macrocycle. The free energy of disulfide formation can be determined by measuring the ratio of reduced to oxidized peptide when in equilibrium with an excess of a reference thiol and its corresponding disulfide, as illustrated in Figure 3 [23,24]. Incubation of samples of a dicysteine-containing peptide under these conditions, followed by an acidic quench of the disulfide exchange and reverse-phase high-pressure liquid chromatography (RP-HPLC) allows measurement of the ratio of reduced to oxidized peptide.

The preparative oxidation of glycopeptide **2a** was slightly slower than that of the corresponding peptide **1a**, probably due to steric hindrance [25]. Incubation of the peptide **1a** and glycopeptide **2a** with glutathione and oxidized glutathione gave relative $K_{eq}$ values of 21 and 38 mM respectively, indicating that it is more favorable for the glycopeptide **2** to be oxidized (and hence cyclic) than for peptide **1** by a ratio of about 1.8:1. This difference amounts to a $\Delta\Delta G$ of about 1.4 kJ $mol^{-1}$. As glycosylation enhances disulfide formation for this peptide, it must change the conformational tendencies of the peptide, bringing the cysteine side chains into closer proximity to each other, and the peptide must adopt a

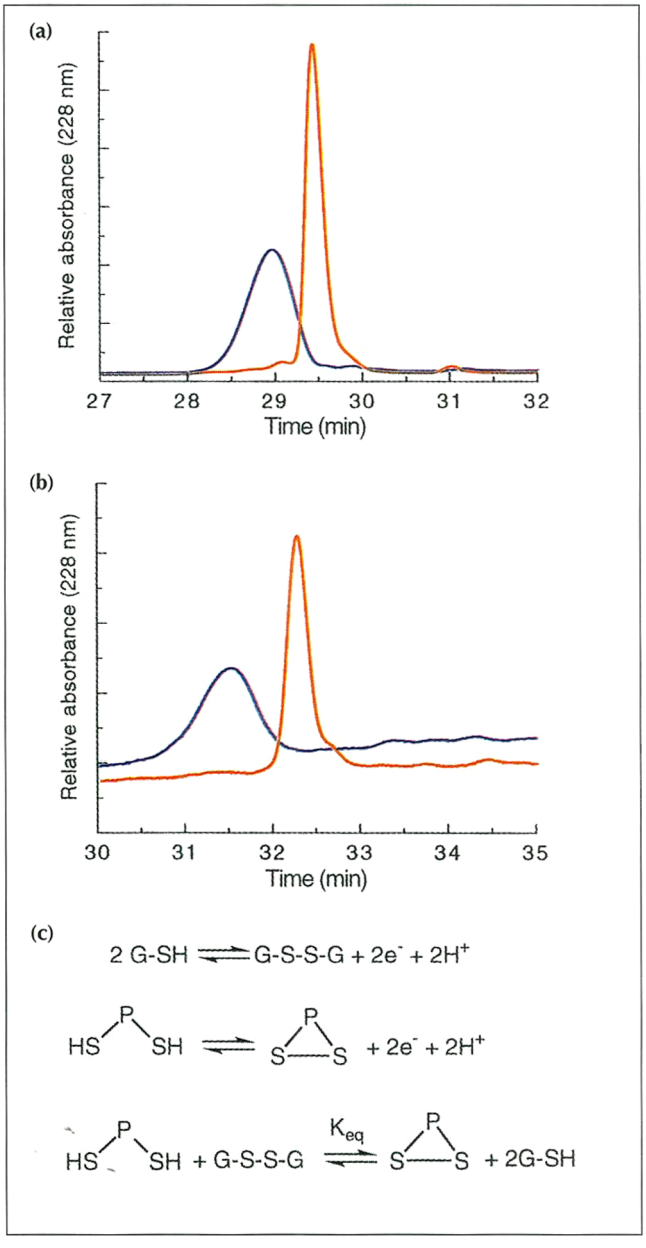


**Fig. 3.** Thermodynamics of disulfide formation. **(a)** Superimposed HPLC traces of the reduced peptide **1a** (red) and the oxidized peptide **1b** (blue). **(b)** Superimposed HPLC traces of the reduced glycopeptide **2a** (red) and the oxidized glycopeptide **2b** (blue). **(c)** Equilibria established between a sample peptide and the reference thiol, glutathione.

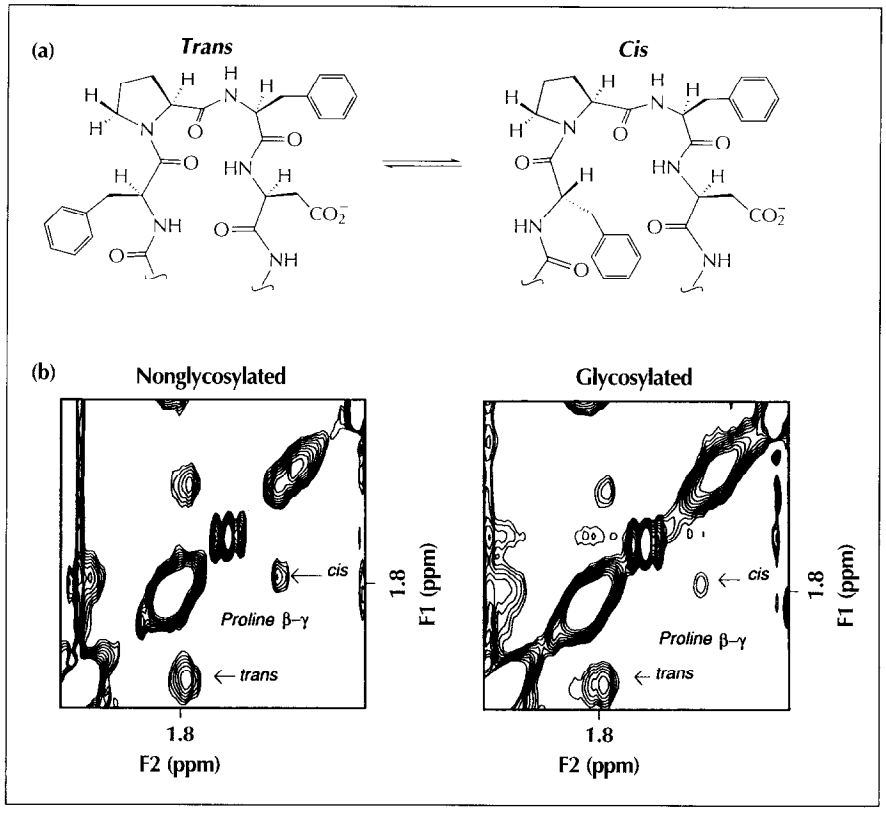


**Fig. 4.** Glycosylation of the loop peptide causes an increase in the proportion of *trans* to *cis* isomer. **(a)** Structural representation of *cis* and *trans* proline amide isomers. **(b)** Two-dimensional NMR TOCSY spectra of the oxidized peptides **1b** and **2b** at pH 4.5, showing a proline β–γ cross-peak of both the *cis* and *trans* isomers.

conformation more consistent with its conformation in the mature, oxidized protein. Although the amount of energy involved is small (1.4 kJ $mol^{-1}$), the thermodynamic stability of a protein is also rather small, and small globular proteins typically have a stability of 32–40 kJ $mol^{-1}$ [26]. If this isolated loop behaves similarly to the peptide sequence when it is part of the protein, then glycosylation is making a measurable contribution to the stability of the whole protein. Additionally, since formation of the correct disulfide bond is often one of the more difficult steps of protein folding [27], glycosylation may make an important contribution to the rate of proper folding of the nAChR α-subunit.

### NMR studies of peptide and glycopeptide: *cis/trans* proline equilibria

NMR analysis of the oxidized glycopeptide **2b** showed that in water, at pH 4.5, the peptide was present as two slowly exchanging conformers, in a ratio of ~2:1. These conformations were attributed to the *cis* and *trans* amide isomers of the proline residue. Chemical shift differences were observed for many of the backbone protons throughout the peptide, but were most pronounced for the proline residue and for the residues in its immediate vicinity. The major conformer was assigned as the *trans*-proline isomer, since it showed the expected $d_{\alpha\delta}$(Phe, Pro) crosspeaks when examined by nuclear Overhauser effect spectroscopy (NOESY) [28]. The absence of these characteristic crosspeaks demonstrated that the other conformer is not a *trans*-proline isomer. The $d_{\alpha\alpha}$(Phe, Pro) and $d_{N\alpha}$(Phe, Pro) crosspeaks associated with *cis* amides were not observed, due to spectral overlap. In this case, it seems reasonable to assign the minor conformer as the *cis*-proline amide.

**Table 2.** *Cis–trans* proline isomer ratios for the oxidized peptide and glycopeptide as determined by one-dimensional NMR.

| Compound | Trans % | Cis % |
|---|---|---|
| Peptide **1b**, pH 4.5 | 55 | 45 |
| Peptide **1b**, pH 7.0 | 58 | 42 |
| Glycopeptide **2b**, pH 4.5 | 70 | 30 |
| Glycopeptide **2b**, pH 7.0 | 75 | 25 |

An examination of two-dimensional $^1H$ spectra of the oxidized, non-glycosylated peptide **1b** also showed the presence of two slowly exchanging conformers, but in this case, at near equal proportions. Again, NOESY spectra confirmed that one conformer contained a *trans* proline, although the limited solubility of peptide **1b** did not allow a full assignment. The chemical shifts for these two conformers, however, were nearly identical to those observed for the oxidized glycopeptide **2b**, allowing assignment of the conformers of the oxidized peptide **1b** as *cis* and *trans* proline isomers. Peptides with aromatic residues immediately preceding proline, such as this sequence, often have significantly enhanced populations of the *cis*-proline conformer [29, 30].

Having identified the two conformers as the *cis* and *trans* proline amide isomers, an interesting question arises regarding protein glycosylation: how does protein glycosylation influence *cis–trans* proline isomerism at a residue that is removed by several residues from the glycosylation

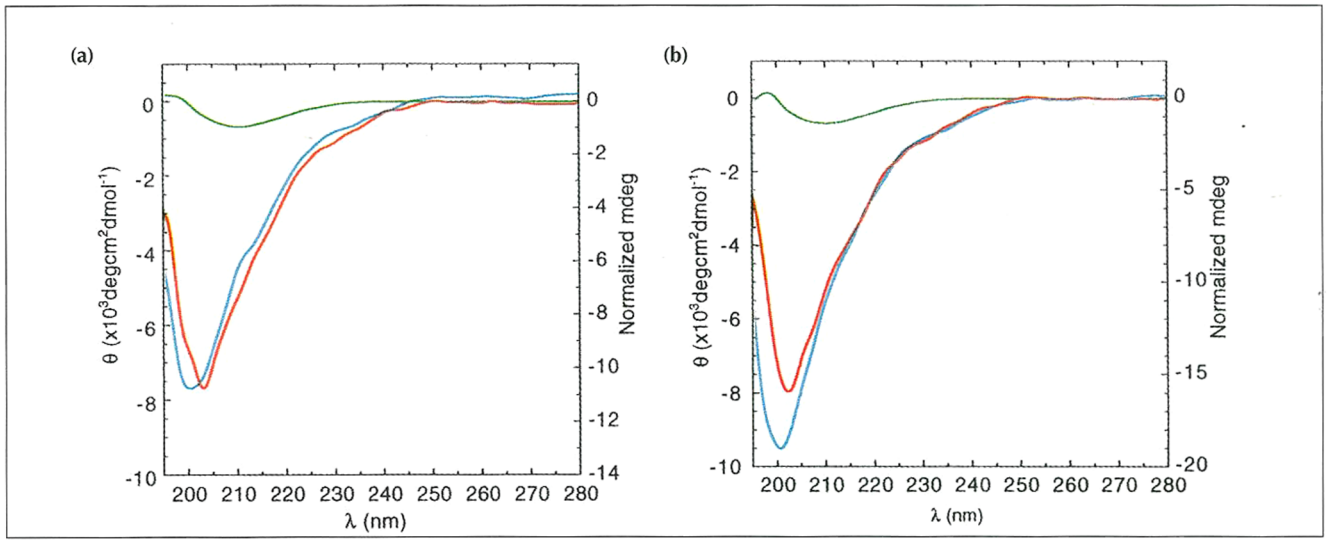


**Fig. 5.** The glycosylated and non-glycosylated peptides have similar CD spectra. The CD spectra of the oxidized peptide **1b** (blue), glycopeptide **2b** (red), and chitobiosylamine (green) at **(a)** pH 4.5 and **(b)** pH 7 are shown. Spectra for the oxidized peptide **1b** and the oxidized glycopeptide **2b** are presented in molar ellipticity units (θ). For comparison, a spectrum of chitobiosylamine, normalized to account for concentration, is presented. All spectra were recorded at room temperature (22 °C).

site in the linear sequence? The *cis/trans* proline isomer ratios were determined for both the oxidized peptide **1b** and the oxidized glycopeptide **2b** using three independent spectroscopic indicators. The ratios were determined from the proline δ–δ and β–γ crosspeaks observed using total correlation spectroscopy (TOCSY) (see Fig. 4). These crosspeaks were distinct, well resolved, and clearly associated with either the *cis* or *trans* conformer. Since the coupling constant between these sets of protons should be relatively constant, the crosspeak volume can be used as a reasonable indicator of species population. Further analysis showed that one threonine methyl resonance in the *cis* conformer was sufficiently well resolved from other resonances to also be used for quantification by integration of one-dimensional spectra. Integration results using both one- and two-dimensional data were very similar and are summarized in Table 2. Whereas raising the pH consistently causes a small increase in the population of the *trans* isomer, glycosylation causes a much larger increase, resulting in the *trans* isomer predominating over the corresponding *cis* isomer. The shift in the equilibrium constant in this case is 1.9:1, corresponding to a $\Delta\Delta G$ of 1.6 kJ mol$^{-1}$. Since these studies were carried out with a truncated disaccharide carbohydrate, it will be interesting to assess whether the effects that we have observed are accentuated with a larger oligosaccharide that more closely reflects the glycosylation product *in vivo*.

Proline *cis–trans* isomerization is important in protein folding and, along with disulfide bond formation, it is considered to be one of the slow steps in the folding process. It is significant that enzymes (peptide prolyl isomerases) exist to catalyze this potentially rate-limiting isomerization [31]. Although it is not yet known which proline amide conformer is found in the intact and mature α subunit, most proline residues in proteins are found in the *trans* form. If this is the case for the α subunit sequence, it would seem unusual that this aromatic–proline site is strongly conserved, unless a mechanism exists for remediating a deleterious proline amide isomer ratio. It seems as if glycosylation is capable of counteracting the inherent tendency of this sequence to adopt the *cis* amide isomer, thereby ensuring proper folding of the mature α subunit. In this regard, the folding behavior of the α-7 variant of this subunit, which forms a homopentameric receptor, is of great interest [32]. The α-7 subunit contains a number of mutations as compared to the *Torpedo* α-1 subunit; in particular, it lacks the glycosylation site that corresponds to Asn142 while still preserving the Phe135-Pro136 sequence. It also possesses significantly more aromatic–proline sub-sequences, predicted to have a high tendency to form the *cis* amide isomer. The folding and assembly of this mutant is dependent on the peptidyl proline isomerase cyclophilin, unlike the heteropentameric receptor containing α-1 [32]. The observations that we have made suggest that the cyclophilin independence of α-1 folding may arise as a consequence of the glycosylation site. Further analysis of these systems will establish whether this postulate is well founded.

*N*-linked glycosylation is clearly an important element in defining the local polypeptide conformation, when the effects on proline amide isomerization are combined with the effects on disulfide bond formation. Glycosylation thus has the potential to influence protein folding by affecting at least two kinetic steps that are considered to be rate-limiting.

### Circular dichroism spectroscopy of the peptide and the glycopeptide

The circular dichroism (CD) spectra for the oxidized peptide **1b**, the oxidized glycopeptide **2b** and chitobiosyl amine at pH 7.0 and at pH 4.5 are shown in Figure 5. Chitobiosylamine was used to estimate the contribution

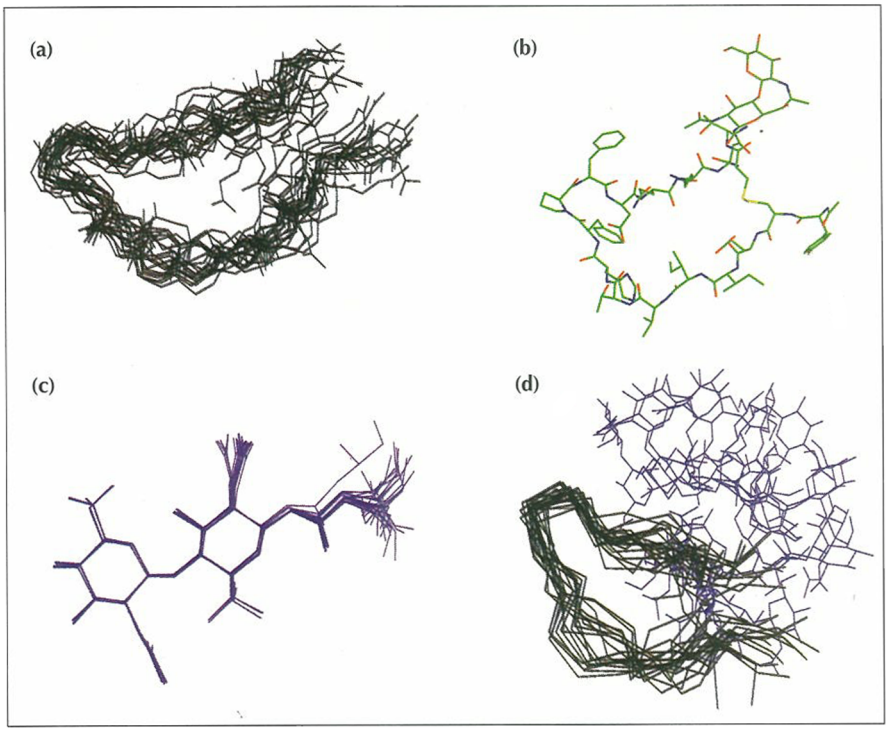


**Fig. 6.** A model of the structure of the oxidized glycopeptide **2b** as determined from NMR. Where the peptide is drawn, the amino terminus is at the lower right, and the carboxyl terminus at the upper right. **(a)** Superimposition of the peptide backbone atoms of the 19 structures with the lowest energy and restraint violations. **(b)** Conformation of lowest energy structure of the oxidized glycopeptide **2b**. **(c)** Superimposition of the disaccharide unit and asparagine residue. **(d)** Superimposition of alpha carbon traces for the peptide of the same 19 structures, with the carbohydrate residues drawn in purple.

of the carbohydrate to the CD spectrum of the glycopeptide. A change in pH has only a small effect on the spectrum of the non-glycosylated peptide, and no readily discernible effect upon the spectra of either the glycopeptide or chitobiosylamine. Both glycopeptide and non-glycosylated peptide have spectra that are similar to each other and to a random coil structure whose residues have either α or β dihedral angles [33]. There is a small shift in the negative ellipticity observed for the glycopeptide to longer wavelengths as compared to the peptide; since this shift is not due to the chitobiosylamine it may indicate a slightly decreased random coil content. CD spectra showed no concentration dependence, demonstrating that aggregation effects are not significant and that the peptide is principally present as a monomer.

### Solution structure of the glycosylated loop peptide

A detailed analysis of the NMR spectra of the oxidized glycopeptide **2b** was carried out to gain additional information on its structure and on the effects of glycosylation. Similar analysis of the oxidized, non-glycosylated peptide **1b** was not possible, because of poor solubility and the high proportion of the *cis*-proline isomer, making spectroscopic assignments ambiguous. For the oxidized glycopeptide, a number of distance and torsional constraints were derived from a series of NOESY spectra, and these were used to determine an NOE restrained simulated annealing structure. Only crosspeaks associated with the *trans*-proline conformer were used to generate these constraints. Thirty-four structures were calculated, and the structures with excessive NOE restraint violations or significantly higher energies than the average were discarded, resulting in a family of 19 structures remaining. These structures all share a common main-chain trace, with an average root mean squared deviation (RMSD) of 1.68 Å from the average structure for backbone atoms of residues 2–16 (see Fig. 6a). The structure formed is a loop, with the proline at the i+1 position of a β-turn, as illustrated in Figure 6b. The carboxy-terminal strand between the disulfide and the β-turn is quite linear. The amino-terminal strand has a distinct bulge around residues 5–8, as might be expected since this section also contains more residues than the carboxy-terminal strand. The terminal residues are much less well defined than those in the macrocycle, with an average RMSD of >4.0 Å. In general, the side-chain conformations are not well defined, with the exception of the cysteines forming the disulfide bond and the two residues that are part of the β-turn. The overall conformation of the peptide is consistent with the CD spectra, which indicated a mixture of random coil and β-sheet structure.

The conformation of the carbohydrate portion of the oxidized glycopeptide **2b** is of particular interest, as we have already demonstrated that this moiety influences both the ease of disulfide bond formation and the equilibrium between *cis* and *trans* proline isomers. The disaccharide is extremely well defined, as can be seen in Figure 6c. However, the NOESY data do not clearly define the torsional angles of the asparagine side chain, due to the lack of long range NOESY crosspeaks between the carbohydrate and the peptide. Simulated annealing performed without such restraints produces RMSD values for the carbohydrate atoms that are extremely high (6–10 Å) when the peptide backbone atoms are superimposed. The location of the carbohydrate with respect to the peptide is thus not well defined, as illustrated in Figure 6d.

In light of the influence of the carbohydrate upon both disulfide formation and *cis–trans* proline isomerization, it

is important to understand exactly how these conformational effects are achieved. As the carbohydrate position with respect to the peptide chain is not well defined, it becomes difficult to invoke a specific interaction that causes these influences. Instead, the carbohydrate might induce these conformational effects by excluding portions of the peptide chain from volumes of space near the glycosylation site. An alternative explanation could be that the carbohydrate alters the microenvironment of the nearby peptide strand, changing its conformational profile. Theoretical studies have suggested that peptide conformation can be highly dependent upon solvent composition [34], and therefore the carbohydrate may act by altering local solvation.

## Significance

**_N_-linked glycosylation is an important part of the protein processing pathway for membrane and secretory proteins in eukaryotic cells and it has a number of effects that ensure proper protein structure and function. In particular, studies have shown that _N_-linked glycosylation is essential for correct and timely folding of some proteins [5,6,35]. Studies with short peptides have shown that _N_-linked glycosylation can perturb the conformational tendencies of these peptides, demonstrating one way by which glycosylation can influence protein folding [7–10]. We have studied the effects of glycosylation upon a peptide representing a loop from the α-subunit of the nicotinic acetylcholine receptor, which has been shown to require glycosylation for folding and assembly.**

**Glycosylation seems to have a significant influence on the conformational tendencies of this peptide. The intramolecular disulfide bond forms more easily in the glycosylated peptide, demonstrating that carbohydrate brings the two ends of the loop into closer proximity, as is the case in the mature protein. Furthermore, in the fully oxidized peptide, glycosylation significantly alters the *cis/trans* proline equilibrium, favoring the *trans* isomer. These results indicate that glycosylation can significantly alter the conformational tendencies of a peptide. Since both disulfide bond formation and *cis/trans* proline equilibria are among the slower steps in the protein folding process, and thus of key importance, it becomes clear that _N_-linked glycosylation has the potential to significantly alter both the course of protein folding and the structure of the mature protein.**

## Materials and methods

### *Peptide synthesis*

Peptides were synthesized using standard Fmoc solid-phase peptide synthesis protocols on a Milligen/Biosearch 9050 automated peptide synthesizer, using a PAL–PEG–PS resin and pre-activated pentafluorophenol esters. The glycopeptide precursor was synthesized with allyl-protected aspartic acid; this residue was coupled using diisopropylcarbodiimide/hydroxybenzotriazole (DIPCDI/HOBt) activation, and all deprotections for this peptide were performed using 0.2 M HOBt in 20 % piperidine, in order to suppress aspartimide formation [36]. All peptides were cleaved using Reagent R (90 % trifluoroacetic acid, 5 % thioanisole, 2 % anisole, 3 % ethanedithiol) for 2 h, then precipitated with ethyl ether. Peptides were then oxidized by incubation in 20 % dimethylsulfoxide (DMSO), pH 7.5, at 0.5 mg $ml^{-1}$ for 12–16 h [37]. After oxidation, the solution was diluted to 10 % DMSO, and loaded onto a C-18 Sep-Pak column, which was then eluted with a series of acetonitrile/water washes, with the proportion of acetonitrile increasing by 5 % per fraction. Sep-Pak fractions were analyzed by HPLC. MALDI-MS 2101.1 $MH^+$.

### *Chemical synthesis of the glycopeptide*

After standard solid-phase peptide synthesis, the allyl ester was deprotected by suspending the resin in a mixture of 37:2:1 chloroform:acetic acid:*N*-methyl morpholine, adding three equivalents of tetrakis(triphenylphosphine) palladium, and incubating for 16 h [16]. After the deprotection, the resin was rinsed with chloroform, 0.5 % diisopropylethylamine in dimethylformamide (DMF), 0.5 % sodium diethyldithiocarbamate in DMF, and DMF. The resin was then treated with a 5-fold excess of hydroxybenzotriazolyl tetramethyluronium hexafluorophosphate (HBTU), HOBt, diisopropylethylamine (DIPEA), and chitobiosylamine for 4–12 h in order to couple the peptide to the carbohydrate [15]. After coupling, the resin was rinsed with DMF, dichloromethane (DCM), and methanol, and dried under vacuum before cleaving. Peptide was cleaved from the resin following the procedures described above. The crude peptide was purified by RP-HPLC to give the pure glycopeptide, and its identity confirmed by mass spectrometry. (MALDI-MS M- 2505). The glycopeptide was then oxidized with DMSO as above. The pure oxidized glycopeptide eluted at ~30 % acetonitrile.

### *Determination of oligosaccharyl transferase kinetics*

Purified peptide samples, dissolved in DMSO, were added to a microcentrifuge tube containing 100 000 dpm of 36.5 Ci $mmol^{-1}$ $^3H$-labeled Dol-PP-GlcNAc-GlcNAc. Assay buffer (30 μl, pH 7.5, 50 mM HEPES, 1.2 % Triton TX-100, 140 mM sucrose, 0.5 mg $ml^{-1}$ phosphatidylcholine, 10 mM $MnCl_2$) was added. Crude pig liver microsomes (200 μl) were suspended in 1.4 ml assay buffer, and 150 μl of this mixture added to each microcentrifuge tube to initiate the enzyme reaction. Aliquots (40 μl) were withdrawn every 20 s and quenched in 1.2 ml 3:2:1 chloroform:methanol:4 mM $MgCl_2$. The aqueous phase was removed, and the organic phase extracted twice with 700 μl theoretical upper phase (12:192:186:2.79 chloroform:methanol:water:0.25 M $MgCl_2$). The combined aqueous phases were scintillation counted using Ecolite(+) (ICN). Reduced peptide **1a** was dissolved in DMSO immediately prior to assaying; under these conditions it was shown that no significant oxidation of the peptide took place before the assay was completed.

### *Enzymatic synthesis of Dol-PP-GlcNAc-GlcNAc*

Several 1.5 ml microcentrifuge tubes were prepared by adding 50 μl of 6 mg $ml^{-1}$ Dolichol-PP-GlcNAc and 33.5 μl 5 mM UDP-GlcNAc to each and evaporating the solvent under nitrogen. For syntheses of radiolabeled Dol-PP-GlcNAc-[$^3H$]-GlcNAc (12 mCi $mmol^{-1}$), 2 μCi UDP-[$^3H$]-GlcNAc was added to each tube. This mixture was then dissolved in 950 μl

of pH 7.0 50 mM Tris/acetate buffer (3 mM DTT, 0.25 M sucrose, 5 mM $MgCl_2$, and 1 % Nonidet NP-40). Pig liver microsomes (50 μl) were added to each tube, which was then shaken for 1–2 h. This mixture was quenched in 10 ml 3:2 chloroform:methanol and 2 ml 4 mM $MgCl_2$. The organic layer was extracted with 6 ml TUP (no salt, 12:192:186 chloroform:methanol:water). After separating the organic layer from the proteinaceous pellet, the pellet was further extracted with 5 ml 3:2 chloroform:methanol. The organic extracts were combined and the solvent removed. This oil was then purified on a column of silica (Kieselgel 60), loaded in 72:21:3 chloroform:methanol:water, then after 35 x 50 drop fractions the product was eluted with 60:25:4 chloroform:methanol:water. Material synthesized without a radiolabel was quantitated by competition assays with radiolabeled material.

### *Enzymatic preparation of glycopeptides*

Twenty microcentrifuge tubes, containing 50 000 dpm of the radiolabeled Dol-PP-GlcNAc-GlcNAc (12 mCi $mmol^{-1}$), or approximately the same amount (1.9 nmol) of unlabeled material, were prepared and 0.1 mg of peptide **1a** in 10 μl DMSO was added to each. To each tube was then added 40 μl of assay buffer (1.2 % Triton-X-100, 0.5 mg $ml^{-1}$ PC, 50 mM HEPES, 140 mM sucrose, 10 mM DTT, 10 mM $MnCl_2$), and then 150 μl micromix (700 μl assay buffer, 100 μl pig liver microsomes). These tubes were prepared and shaken for 3 h, then quenched into 20 ml 3:2 chloroform:methanol and 4 ml 4 mM $MgCl_2$. After separating phases, the organic phase was extracted with 14 ml TUP (12:192:186:2.79 chloroform:methanol:water:0.25 M $MgCl_2$). The combined aqueous phases were blown down or centrifuged under vacuum to remove the organic solvents, and then purified using Sep-Pak columns, eluting in 3 ml of 5 % incremented acetonitrile content. The glycopeptide **2a** eluted during the 25–30 % acetonitrile fractions, and was then further purified by HPLC, using an analytical C18 column and a 15–40 % acetonitrile gradient. The identity of the purified glycopeptide was confirmed by mass spectrometry. (MALDI-MS $MH^+$ 2506).

### *Thermodynamics of disulfide formation*

Peptide disulfide thermodynamics were established by incubating a 50 μM or less solution of the peptide with 2.4 mM oxidized glutathione and 7.15 mM reduced glutathione, in a 0.1 M Tris, pH 8.5 buffer, with 1 mM EDTA. After 2 h of incubation, several aliquots were analyzed by HPLC, using an analytical C18 column and a 25–40 % acetonitrile gradient for the nonglycosylated peptide. A 15–40 % gradient was used for the glycopeptide as its retention times had already been characterized with that gradient. Reduced and oxidized peptide peaks were either quantitated using their UV absorbance, corrected for changes in UV absorbance due to the disulfide bond, or in the case of the glycopeptide, based on $^3H$ label. Both methods gave similar results. Equilibria were calculated from the average of several such measurements.

### *Circular dichroism spectroscopy*

Samples were prepared at 100–150 μM in unbuffered, pH adjusted, degassed water. CD spectra were invariant from 600 to 40 μM (data not shown). Spectra were acquired from 280 to 195 nm at room temperature on a Jasco J600 spectrometer and averaged over 8 scans. Spectra of peptides were converted to molar ellipticities; spectra of chitobiosylamine were converted to normalized millidegrees. Peptide concentrations were calculated from the unique tyrosine absorbance ($\lambda_{max}$ 278 nm; $\epsilon_{max}$ 1100), chitobiosylamine concentrations were based on weight.

### *NMR spectroscopy*

NMR samples were dissolved in 90 % $H_2O$, 10 % $D_2O$ and the pH was adjusted to 4.5. Most NMR spectra were acquired on a Varian 600 MHz NMR spectrometer; data were subsequently processed using Felix 2.3.0 (Biosym Technologies, San Diego, CA) and analyzed using Felix and Pronto 3D^2 [38]. Additional spectra were acquired at pH 7.0, in 100 % $D_2O$, or using a Bruker AMX 500 MHz NMR spectrometer as necessary. Water suppression was achieved either using presaturation of the water resonance during the relaxation delay, or a WATERGATE pulse sequence [39]. Spin systems were principally assigned from a TOCSY spectrum [40,41]. *Cis/trans* proline ratios were determined by integration of the Thr7 methyl peak at 1.08 ppm which is associated with the *cis* isomer only, and comparing it with the integration of the valine/isoleucine methyl peaks from 0.97–0.83 ppm as representative of both isomers.

### *Structure generation*

NOESY crosspeak intensities were measured on a series of NOESY [42] spectra taken with 100 ms, 200 ms and 300 ms mixing times. Additional crosspeak intensities, for crosspeaks obscured by residual water signals, were measured using a $D_2O$ NOESY taken with a 200 ms mixing time, and from WATERGATE NOESY spectra at 200 ms and 300 ms mixing times. Crosspeak intensities were compared with a number of β–β crosspeaks of known internuclear distance. Using buildup rates derived from a linear fit of the crosspeak volumes versus mixing times, or a single mixing time calculation for the crosspeaks observed only in the $D_2O$ spectrum, interproton distances were calculated and these distances were sorted into three classes: short, medium and long. These distances were then used to produce distance restraints for simulated annealing of 1.0–2.5 Å, 1.8–3.5 Å, and 1.8–5.0 Å for the short, medium, and long classes respectively. Standard pseudo-atom corrections were applied [28]. Dihedral restraints, consistent with the NOESY crosspeak data indicating *trans*-amide bonds, were placed upon the proline amide bond, and upon each of the amide bonds associated with each of the acetyl groups. These restraints were then used in a simulated annealing protocol, as described by Nilges *et al.* [43] using NMRchitect (Biosym Technologies, San Diego, CA). Thirty-four structures were generated, of which 15 with energies or NMR restraint violations significantly above the average were discarded.

*Acknowledgements:* We thank Professor Henry Lester and Professor Dennis Dougherty for helpful discussions and Mary Struthers for assistance with NMR spectroscopy. We acknowledge the Dorothy Chandler, Camilla Chandler Frost Laboratory in Biology for use of NMR instrumentation. This research was supported by National Institutes of Health grant GM 39334 and a Fannie and John Hertz predoctoral fellowship (to K.W.R.). B.I. also acknowledges support from the Alfred P. Sloan Foundation and the Camille and Henry Dreyfus Teacher Scholar Program.

## References

1. Imperiali, B. & Hendrickson, T.L. (1995). Asparagine-linked glycosylation: specificity and function of oligosaccharyl transferase. *Bioorg. Med. Chem.*, in press.
2. Rudd, P.M., *et al.*, & Dwek, R.A. (1994). Glycoforms modify the dynamic stability and functional activity of an enzyme. *Biochemistry* **33**, 17–22.
3. Joao, H.C., Scragg, I.G. & Dwek, R.A. (1992). Effects of glycosylation on protein conformation and amide proton exchange rates in RNase B. *FEBS Lett.* **307**, 343–346.
4. Wyss, D.F., *et al.*, & Wagner, G. (1995). Conformation and function of the *N*-linked glycan in the adhesion domain of human CD2. *Science* **269**, 1273–1278.

5. Duranti, M., Gius, C., Sessa, F. & Vecchio, G. (1995). The saccharide chain of lupin seed conglutin γ is not responsible for the protection of the native protein from degradation by trypsin, but facilitates the refolding of the acid-treated protein to the resistant conformation. *Eur. J. Biochem.* **230**, 886–891.
6. Riederer, M.A. & Hinnen, A. (1991). Removal of *N*-glycosylation sites of the yeast acid phosphatase severely affects protein folding. *J. Bacteriol.* **173**, 3539–3546.
7. Otvos, L., Thurin, J., Kollat, E., Urge, L., Mantsch, H.M. & Hollosi, M. (1991). Glycosylation of synthetic peptides breaks helices. *Int. J. Pept. Protein Res.* **38**, 476–482.
8. Imperiali, B. & Rickert, K.W. (1995). Conformational implications of asparagine-linked glycosylation. *Proc. Natl. Acad. Sci. USA* **92**, 97–101.
9. Wormald, M.R., *et al.*, & Dwek, R.A. (1991). The conformational effects of N-glycosylation on the tailpiece from serum IgM. *Eur. J. Biochem.* **198**, 131–139.
10. Andreotti, A.H. & Kahne, D. (1993). Effects of glycosylation on peptide backbone conformation. *J. Am. Chem. Soc.* **115**, 3352–3353.
11. Green, W.N. & Millar, N.S. (1995). Ion-channel assembly. *Trends Neurosci.* **18**, 280–287.
12. Gehle, V.M. & Sumikawa, K. (1991). Site-directed mutagenesis of the conserved *N*-glycosylation site on the nicotinic acetylcholine receptor subunits. *Mol. Brain Res.* **11**, 17–25.
13. Blount, P. & Merlie, J.P. (1990). Mutational analysis of muscle nicotinic acetylcholine receptor subunit assembly. *J. Cell Biol.* **111**, 2613–2622.
14. Mishina, M., *et al.*, & Numa, S. (1985). Location of functional regions of acetylcholine receptor α-subunit by site-directed mutagenesis. *Nature* **313**, 364–369.
15. Cohen-Anisfeld, S.T. & Lansbury, P.T. (1993). A practical, convergent method for glycopeptide synthesis. *J. Am. Chem. Soc.* **115**, 10531–10537.
16. Kates, S.A., de la Torre, B.G., Eritja, R. & Albericio, F. (1994). Solid-phase *N*-glycopeptide synthesis using allyl side-chain protected Fmoc-amino acids. *Tetrahedron Lett.* **35**, 1033–1034.
17. Imperiali, B., Shannon, K.L. & Rickert, K.W. (1992). Role of peptide conformation in asparagine-linked glycosylation. *J. Am. Chem. Soc.* **114**, 7942–7944.
18. Imperiali, B., Spencer, J.R. & Struthers, M.D. (1994). Structural and functional characterization of a constrained Asx-turn motif. *J. Am. Chem. Soc.* **116**, 8424–8425.
19. Nilsson, I. & von Heijne, G. (1993). Determination of the distance between the oligosaccharyltransferase active site and the endoplasmic reticulum membrane. *J. Biol. Chem.* **268**, 5798–5801.
20. Pless, D.D. & Lennarz, W.J. (1977). Enzymatic conversion of proteins to glycoproteins. *Proc. Natl. Acad. Sci. USA* **74**, 134–138.
21. Bergman, L.W. & Kuehl, W.M. (1978). Temporal relationship of translation and glycosylation of immunoglobulin heavy and light chains. *Biochemistry* **17**, 5174–5180.
22. Sumikawa, K. & Gehle, V.M. (1992). Assembly of mutant subunits of the nicotinic acetylcholine receptor lacking the conserved disulfide loop structure. *J. Biol. Chem.* **267**, 6286–6290.
23. Falcomer, C.M., *et al.*, & Scheraga, H.A. (1992). Chain reversals in model peptides: studies of cystine-containing cyclic peptides. 3. Conformational free energies of cyclization of tetrapeptides of sequence Ac-Cys-Pro-X-Cys-NHMe. *J. Am. Chem. Soc.* **114**, 4036–4042.
24. Lin, T.-Y. & Kim, P.S. (1989). Urea dependence of thiol-disulfide equilibria in thioredoxin: confirmation of the linkage relationship and a sensitive assay for structure. *Biochemistry* **28**, 5282–5287.
25. Urge, L., Jackson, D.C., Gorbics, L., Wroblewski, K., Graczyk, G. & Otvos, L. (1994). Synthesis and conformational analysis of *N*-glycopeptides that contain extended sugar chains. *Tetrahedron* **50**, 2373–2390.
26. Creighton, T.E. (1984). *Proteins: Structures and Molecular Principles.* W.H. Freeman and Co., New York.
27. Freedman, R.B., Bulleid, N.J., Hawkins, H.C. & Paver, J.L. (1989). Role of protein disulphide isomerase in the expression of native proteins. *Biochem. Soc. Symp.* **55**, 167–192.
28. Wüthrich, K. (1986). *NMR of Proteins and Nucleic Acids.* John Wiley and Sons, New York.
29. Grathwohl, C. & Wüthrich, K. (1976). The X-Pro peptide bond as an NMR probe for conformational studies of flexible linear peptides. *Biopolymers* **15**, 2025–2041.
30. Yao, J., Feher, V.A., Espejo, B.F., Reymond, M.T., Wright, P.E. & Dyson, H.J. (1994). Stabilization of a type VI turn in a family of linear peptides in water solution. *J. Mol. Biol.* **243**, 736–753.
31. Schmid, F.X., Mayr, L.M., Mücke, M. & Schönbrunner, E.R. (1993). Prolyl isomerases: role in protein folding. *Adv. Protein Chem.* **44**, 25–66.
32. Helekar, S.A., Char, D., Neff, S. & Patrick, J. (1994). Prolyl isomerase requirement for the expression of functional homo-oligomeric ligand-gated ion channels. *Neuron* **12**, 179–189.
33. Woody, R.W. (1995). Circular dichroism. *Methods Enzymol.* **246**, 34–71.
34. Perkyns, J.S. & Pettitt, B.M. (1995). Peptide conformations are restricted by solution stability. *J. Phys. Chem.* **99**, 1–2.
35. Marquardt, T. & Helenius, A. (1992). Misfolding and aggregation of newly synthesized proteins in the endoplasmic reticulum. *J. Cell Biol.* **117**, 505–513.
36. Dölling, R., *et al.*, & Bienert, M. (1994). Piperidine-mediated side product formation for Asp(OBu$^t$)-containing peptides. *J. Chem. Soc., Chem. Commun.*, 853–854.
37. Tam, J.P., Wu, C.-R., Liu, W. & Zhang, J.-W. (1991). Disulfide bond formation in peptides by dimethylsulfoxide. Scope and applications. *J. Am. Chem. Soc.* **113**, 6657–6662.
38. Kjaer, M., Andersen, K.V. & Poulsen, F.M. (1994). Automated and semi-automated analysis of homo- and hetero-nuclear multi-dimensional NMR spectra of proteins. *Methods Enzymol.* **239**, 288–307.
39. Piotto, M., Saudek, V. & Sklenàr, V. (1992). Gradient-tailored excitation for single-quantum NMR spectroscopy of aqueous solutions. *J. Biomol. NMR* **2**, 661–665.
40. Bax, A. & Davis, D.G. (1985). MLEV-17-based two-dimensional homonuclear magnetization transfer spectroscopy. *J. Magn. Reson.* **65**, 355–360.
41. Griesinger, C., Otting, G., Wüthrich, K. & Ernst, R.R. (1988). Clean TOCSY for $^1$H spin system identification in macromolecules. *J. Am. Chem. Soc.* **110**, 7870–7872.
42. States, D.J., Haberkorn, R.A. & Ruben, D.J. (1982). A two-dimensional nuclear Overhauser experiment with pure absorption phase in four quadrants. *J. Magn. Reson.* **48**, 286–292.
43. Nilges, M., Clore, G.M. & Gronenborn, A.M. (1988). Determination of three-dimensional structures of proteins from interproton distance data by dynamical simulated annealing from a random array of atoms. *FEBS Lett.* **239**, 129–136.


Received: **4 Oct 1995**. Accepted: **18 Oct 1995**.